http://ansinet.com/itj

ITJ

ISSN 1812-5638

INFORMATION TECHNOLOGY JOURNAL

ANSInet
Asian Network for Scientific Information
308 Lasani Town, Sargodha Road, Faisalabad - Pakistan

Information Technology Journal 10 (9): 1709-1716, 2011
ISSN 1812-5638 / DOI: 10.3923/itj.2011.1709.1716

An Improved Method for Robust Blur Estimation

Xianyong Fang, Hao Wu, Zhongbiao Wu and Bin Luo
School of Computer Science and Technology, Anhui University, Hefei 230039, China

Abstract: Linear motion blur estimation is widely studied in the ill-posed deblur related research, but existing methods are too complex, inaccurate or unstable. This study proposes an improved method with two novel contributions to former frequency based method. One is a novel preprocessing step consisting of Hann windowing and histogram equalization. Hann windowing is used to remove the boundary artifacts in the log spectrum while histogram equalization is used to enhance the contrast of the log spectrum. The other is an improved Hough transform based method to estimate the blur direction with cepstrum which eliminates the effect of noise. The method incorporates a least squares line fitting into the traditional Hough transform, and thus accurately estimates the direction. Experimental results demonstrate the efficiency of the proposed method.

Key words: Linear motion blur, preprocessing step, hann windowing, histogram equalization, cepstrum, Hough transform, least squares line fitting

INTRODUCTION

Blur is a common degradation phenomenon in the imaging process and has been studied for many years (Richardson, 1972; Qureshi *et al*., 2003). It is still very difficult today as an ill-posed problem (Cai *et al*., 2010; Whyte *et al*., 2010; Yu *et al*., 2010; Bai *et al*., 2008). Some researches focused on the simplified linear motion blur (Yitzhaky and Kopeika, 1997; Dobes *et al*., 2010) which greatly relieves the complexity of blur estimation. We are also interested in this tactic and propose an improved method in this study.

Perhaps the most successful work in the linear motion blur estimation is the frequency based method where the blur kernel is estimated with Fourier transform (Cannon, 1976). This method inspects zero patterns of the blurred image in the spectral domain and is the basis of many researches later on. Rekleitis (1995) improved this idea with the motion direction estimation by the second derivative of the Gaussian filter and the motion magnitude estimation by the cepstrum analysis. Some complex preprocessing steps such as windowing and zero-padding are also used. This method is also adopted by Schoueri *et al*. (2009) to estimate the piece-wise optical flow (Iffa *et al*., 2011). The problem of Rekleitis is that the second derivative of the Gaussian filter is unstable in finding maximum direction corresponding to the blur direction. In addition, the complex preprocessing is unnecessary for most images.

Moghaddam and Jamzad (2007) also extended Cannon with Radon transform to estimate the motion direction and bi-spectrum modeling to find the motion length. But Radon transform in the spatial domain is very unstable. In addition, its result is rough, or it will be very complicated if we want to obtain a very accurate angle i.e., a lot of angles have to be specified explicitly if a high detection precision is expected. Ji and Liu (2008) further extended this idea to gradient domain and proposed a hybrid Fourier-Radon transform for blur estimation. Gradient domain is also sensitive to noise. Recently, Lokhande *et al*. (2006) proposed Hough transform to compute the blur kernel. Hough transform is adopted in the log spectrum of the blurred image in this study which may be unstable when there are many dark lines corresponding to the blur direction. In addition, similar to Radon transform, Hough transform is also very complicated for a high precision detection (Yu *et al*., 2008). However, Hough is more flexible than Radon. Therefore, Hough transform is adopted by us and improved in our work for the easy and accurate direction estimation.

Some other researches try the non-frequency solution. Yitzhaky and Kopeika (1997) estimated the direction and extension using the Autocorrelation Function (ACF) of the image derivatives. Rav-Acha and Peleg (2005) estimated two blurred image simultaneously though mutual re-blurring. Recently, Dai and Wu (2008) used alpha channel to estimate motion. Similar idea is also adopted by Boracchi *et al*. (2008). But in the blurred area alpha is ambiguous for foreground and background and thus this method is unstable.

In this study, we propose an improved frequency based method. Our contribution lies in two aspects:

Corresponding Author: Xianyong Fang, School of Computer Science and Technology, Anhui University, Hefei 230039, China

- A new simple preprocessing step consisting of Hann windowing and histogram equalization is presented with the former for anti-artifacts and the latter for contrast enhancement
- Hough transform based on the cepstrum of the blurred image is adopted and improved with an additional least squares line fitting for accurate estimation of the motion direction efficiently

THE PRINCIPLE OF LOG SPECTRUM BASED BLUR ESTIMATION

The blur model: The blurred image g (x, y) is generated due to the corruption of a blur kernel h (x, y) to the clear or latent image f (x, y) and noise n (x, y):

$$g(x, y) = f(x, y) * h(x, y) + n(x, y) \quad (1)$$

where * represents convolution. For the linear motion blur, its general form is as the following Lagendijk and Jan (2005).

$$h(x,y) = \begin{cases} \frac{1}{L} & \text{if } \sqrt{x^2 + y^2} \le \frac{L}{2} \text{ and } \frac{x}{y} = -\tan(\varphi) \\ 0 & \text{otherwise} \end{cases}$$

where, L is the motion length and ϕ is the motion direction. The purpose in this paper is to estimate the two-tuple L, ϕ represented blur kernel.

The principle of power spectrum based blur estimation: If taking Fourier transform of Eq. 1 without considering the noise, we have:

$$G(u, v) = F(u, v)\, H(u, v) \quad (2)$$

where, G (u, v), F (u, v) and H (u, v) are the Fourier transform of g (x, y), f (x, y) and h (x, y), respectively.

Alternatively, if we consider the movement of the camera during capturing time T in horizontal (x) and vertical (y) directions being x (t) and y (t), we obtain:

$$g(x,y) = \int_0^T f(x - x(t), y - y(t))\, dt \quad (3)$$

Applying Fourier transform to Eq. 3 yields:

$$\begin{aligned} G(u,v) &= \int\int_{-\infty}^{\infty} [\int_0^T f(x - x(t), y - y(t))\, dt] e^{-j2\pi(ux+vy)} dxdy \\ &= \int_0^T [\int\int_{-\infty}^{\infty} f(x - x(t), y - y(t))\, e^{-j2\pi(ux+vy)} dxdy]\, dt \\ &= F(u,v) \int_0^T e^{-j2\pi(ux+vy)} dt \end{aligned} \quad (4)$$

Therefore, it can be observed from Eq. 2 and 4 that:

$$H(u,v) = \int_0^T e^{-j2\pi(ux+vy)} dt \quad (5)$$

If the movement distance during T in the x and y directions are a and b, respectively, i.e., x (t) = / T and y (t) = bt / T, Eq. 5 turns into:

$$H(u,v) = \frac{T \sin(\pi(ua + vb))}{\pi(ua + vb)} e^{-j\pi(ua+vb)} \quad (6)$$

The solution of above equation is also the parameters of the blur kernel since A = lCOS (ϕ) and B = lSIN (ϕ).

Assuming θ = ucos (ϕ) + vsin (ϕ) and s = W/L where W is the width of the image, we can rewrite Eq. 6 as:

$$H(u,v) = \frac{T \sin(\pi\theta / s)}{\pi\theta / s} e^{-j\pi\theta/s} \quad (7)$$

It can be seen that h (u, v) as well as G (u, v) equal zero when θ = s, 2s, ..., ms. If the log spectrum of the blurred image, LOGS (u, v) , is defined as:

$$LOGS(u,v) = \log(1 + |G(u,v)|) \quad (8)$$

this phenomenon is shown as equally and parallel spaced dark lines in LOGS (u, v) where the distance between neighboring lines, s , is inversely proportional to L .

Therefore, the log spectrum can be used to compute the blur kernel. In the following, we discuss the proposed estimation method in detail.

THE IMPROVED BLUR ESTIMATION METHOD

Our proposed method consists of three steps: Preprocessing, blur direction estimation and blur length estimation. In the preprocessing, Hann windowing and Histogram equalization are used to remove sudden changes along the borders and enhance the contrast of the log spectrum. The blur direction estimation is done with the improved Hough transform of the cepstrum and the blur length estimation is fulfilled with collapsed 1D log spectrum.

Preprocessing: Two sub-steps are adopted as we discussed before: Hann windowing and histogram equalization.

Hann windowing: The Fourier transform treats data as being infinite and thus obtains an infinite periodic signal. But the real image is limited in size and there will be boundary effects (artifacts) in the frequency content. One needs to modify the original signal with a weighting (windowing) function to eliminate the effect of the sudden

changes along the borders. Therefore, windowing function is adopted first to remove the boundary artifacts in the spectrum.

There are several popular windowing functions such as Hann, Hamming, Tukey, Lanczos and Gaussian windows. In our study, Hann function is used because it is very low aliasing which is formulated as:

$$w(n) = 0.5\,(1 - \cos(\frac{2\pi n}{C-1})) \tag{9}$$

where, $n \in \{0, 1, ..., C-1\}$ with C being the width of the window function.

Histogram equalization: After removing the boundary artifacts through windowing, we also adopt histogram equalization to enhance the dark lines and improve the contrasts of the log spectrum. The basic idea of histogram equalization is to re-distribute the intensities on the histogram so that low local contrast areas will gain a higher contrast. The key to such an equalization process is the transformation function which will be discussed below.

In the histogram equalization, first the probability density function of the source image for each intensity l, $p_0(l)$, is computed and then the Cumulative Distribution Function (CDF) for each intensity l is obtained by:

$$CDF_0(l) = \sum_{j=0}^{l} p_0(j) \tag{10}$$

This cumulative distribution is the transformation function which can generate an output image whose intensity levels are equally likely and cover the whole intensity range Gonzalez and Woods (2007). The interesting property of this intensity-level equalization process is that the output image will have an increased dynamic range with a higher contrast than that of the source image. Therefore, Eq. 10 is adopted to construct the histogram equalized log spectrum for blur direction and length estimations.

Direction estimation: Now we discuss how to compute the blur direction. The traditional Hough transform for blur estimation works in the log spectrum of the blurred image but it might be weak due to the noise around multiple dark lines. We step further to perform Hough transform with the Fourier transform of the log spectrum, i. e., cepstrum.

First the cepstrum image is transformed into a binary image and then the Hough transformation is applied to find the best intersect line for all possible lines passing each pixel. A line passing each pixel is normally formulated as $r = x\cos\alpha + y\sin\alpha$ where r and α represent the distance of the line to the origin and the angle of the line to x axis. However, Hough transform normally can only return a regular direction according to the pre-defined angle step, so its result is rough. To remove this limit, we propose a new method for estimating the accurate direction.

In our method, Hough transform is used first for finding the pixel set that voting the true blur direction. Then the blur direction is re-estimated with the set. We adopt a least squares approach with the voted pixels. The dark line and the position of the voted pixel are defined as and (x_i, y_i), respectively. The least squares method finds the optimum and by minimizing the sum of the squared residuals of the total q pixels:

$$\varepsilon = \sum_{i=1}^{q} (y_i - (mx_i + b))^2 \tag{11}$$

Equation 11 is a typical linear least squares problem and its unique solution can be obtained by solving the normal equations:

$$X\beta = Y \tag{12}$$

where:

$$\mathbf{X} = \begin{pmatrix} x_1 & 1 \\ x_2 & 1 \\ \vdots & \vdots \\ x_q & 1 \end{pmatrix}$$

$$\beta = \begin{pmatrix} m \\ b \end{pmatrix}$$

and

$$\mathbf{Y} = \begin{pmatrix} y_1 \\ y_2 \\ \vdots \\ y_q \end{pmatrix}$$

The blur direction can be computed with directly after solving Equation 12 using $\beta = (X^T X)^{-1} X^T Y$.

Blur length estimation: The blur length is estimated after obtaining the blur direction. The log spectrum is first inversely rotated according to the direction and then projected to the x- axis to obtain a collapsed 1D spectrum. The local minima correspond to the dark line

positions which are spaced with almost the same distance. Detecting those minima and averaging the distances between them as s, we can compute the final blur length by L= W/s.

RESULTS

We now discuss the experimental results which are implemented by MATLAB 7.5. In the experiments, the threshold of the cepstrum binarization is 0.35, the minimum distance between two local minima for length estimation is 20 and the angle step in Hough transform is 1.

Figure 1 demonstrates the principle of the power spectrum based blur estimation. In Fig. 1, blurred Lena images and corresponding log spectra are computed with different blur kernels. There is no dark line in the spectrum of the clear image but there are significant lines in those of the blurred images which are perpendicular to their corresponding blur directions. We can also see that the larger the blur width, the smaller the line distance.

Figure 2 a-f show the preprocessing step. The log spectrum of blurred Lena Fig. 2a before windowing Fig. 2b contains significant boundary artifacts (horizontal and vertical bright signals). But they do not exist after windowing Fig. 2c. Apparently direct processing the log spectrum Fig. 2b will lead to ambiguous blur kernels, i.e., horizontal and vertical bright signals may be taken as the responses of the horizontal and vertical blur kernels, respectively.

For the other sub-step, histogram equalization, we can see from Fig. 2 that the color intensities are more evenly distributed after equalization Fig. 2f than before Fig. 2e. The contrast of the whole spectrum image is enhanced significantly for further blur estimation (Fig. 2d, c).

Figure 3 shows the process of Hough transform for detecting blur detection. The cepstrum of the Lena image (Fig. 3a) is first transformed into binary format (Fig. 3b) and then the rough blur direction is obtained from the line voted by the largest number of pixels according to Hough transform. Figure 3c shows the pixels that are corresponding to the detected line direction (26 degree). The linear least squares line fitting is then applied to those pixels and the angle finally obtained is 25.4218 degree which is closer and more accurate to the true direction (25 degree) than the direction estimated by Hough (26 degree).

More experiments with different blur kernels are also undertaken (Table 1) where the blur directions are equally separated by 5 degrees and the blur lengths are randomly selected. (35, 15) and (17, 45) get the minimum error of estimated length (0.0316) and the minimum error of estimated direction (0.0000), respectively. We can also see from this Table 1 about half of blur lengths can be estimated with an error below 0.1; 2), about half of blur directions can be estimated with an error below 0.5 and 3. There is no length error bigger than 0.4 and no angle error bigger than one. These experiments show that both length and angle can be obtained robustly for all differently blurred images with our proposed method.

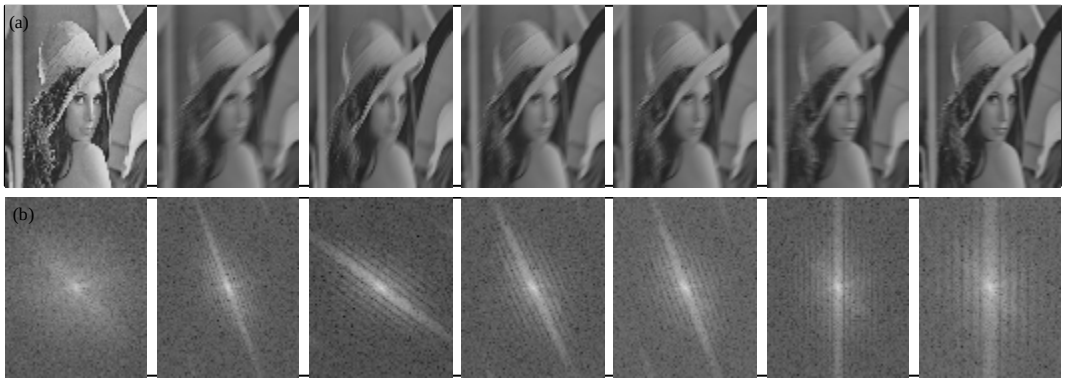

Fig. 1 (a-b): The log spectra of differently blurred Lena image, The clear image and its blurred series. The left most image is the clear image and others are the blurred images with different blurs. From left to right, the blur kernel are (35,25), (25,60), (25,30), (25,25), (25,0) and (15,0), respectively, (b) The log spectra corresponding to the images shown in Fig. 1a

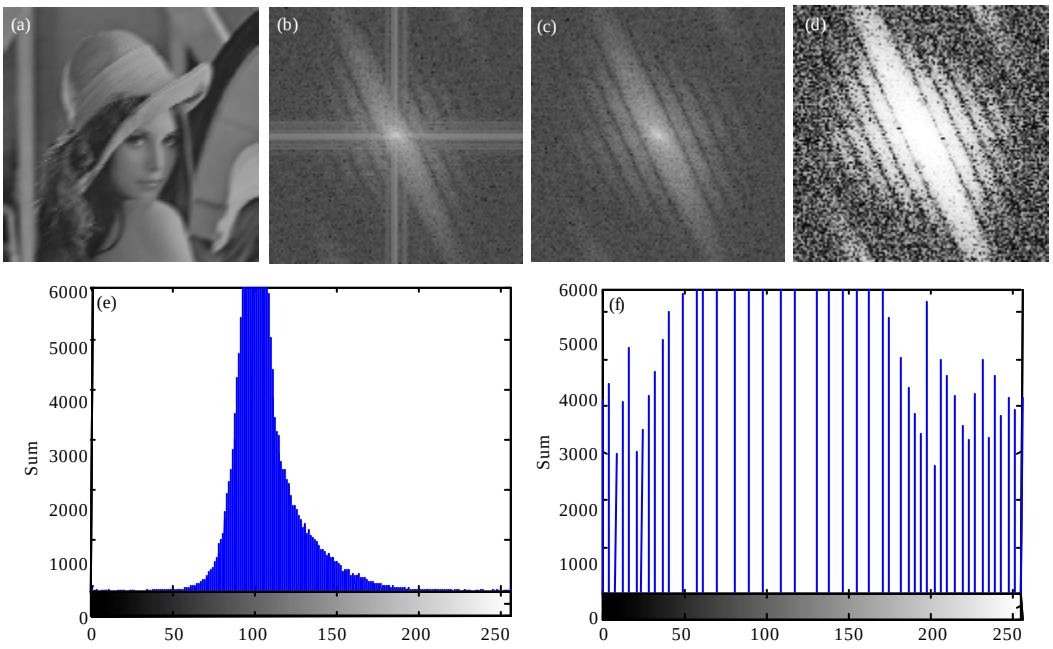

Fig. 2 (a-f): The preprocessing step of the Lena blurred with the blur kernel (15, 25); (a) the blurred image, (b) the log spectrum of Fig. 2a before Fig. 2e windowing, (c) the log spectrum of Fig. 2a after windowing. There is no histogram equalization, (d) the log spectrum of Fig. 2c after histogram equalization, (e) the histogram of Fig. 2d the histogram

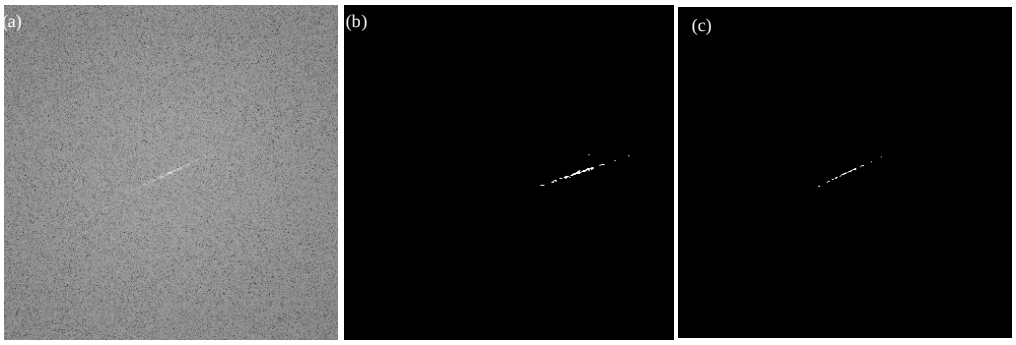

Fig. 3 (a-c): Hough transform for blur direction detection in Fig. 2a. The angle after the least squares fitting is 25.4218 degree; The cepstrum of the blurres image, (b) the binary image of Fig. 3a and c the pixels on the votes line (26 degree) after Hough transform of Fig. 3b

Additional experiments are taken for the cameraman and livingroom (Fig. 5). The experiments use the same blur kernels as Table 1 and their results are shown in Table 2 and 3, respectively. All length errors are below 0.4 for both images. Especially, livingroom achieves better performance than cameraman and Lena (The length estimation errors of livingroom are all below 0.3). The possible reason is that livingroom is more textured than cameraman and Lena and thus its local minima can be more robustly obtained than the less textured cameraman and Lena. Table 2 and 3 that each image has only one blur estimated with an error bigger than 0.5. This property shows both cameraman and livingroom obtain higher direction estimation accuracies than Lena.

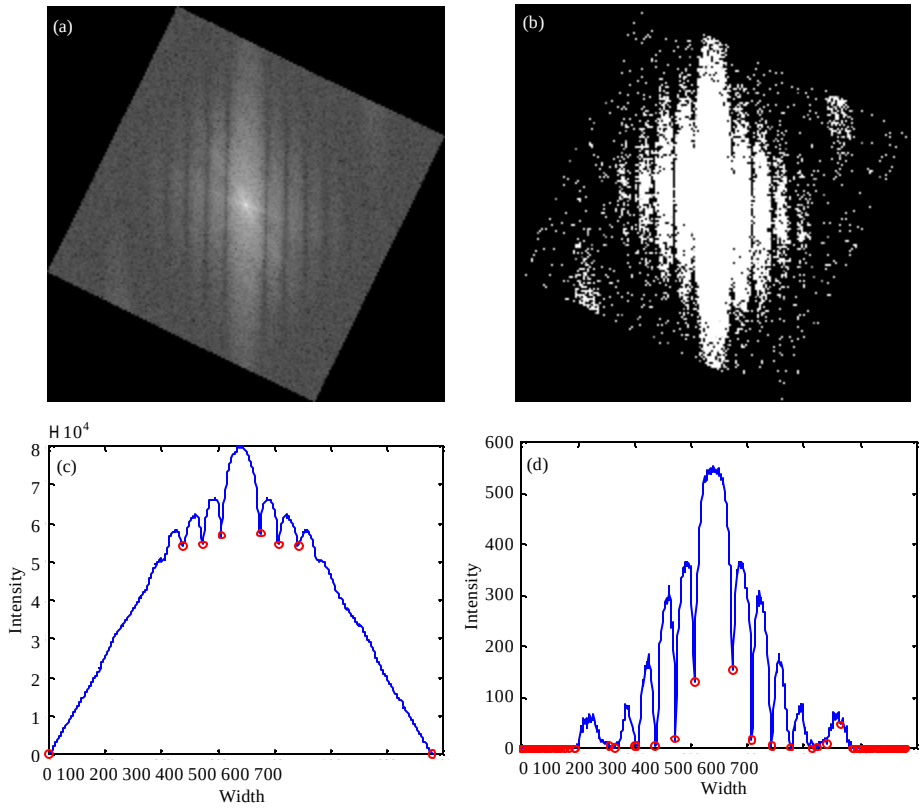

Fig. 4 (a-d): Blur length computation for the blurred image in Fig. 2a. (a) The rotated log spectrum according to the detected blur direction (25.4218 degree), (b) The binary image of Fig. 4a, (c) Te collapsed ID spectrum of Fig. 4a, the red circles show the local minima detected and the blur length computed is 14.9851 and (d) The collapsed ID spectrum of Fig. 4a, the red circles show the local minima detected and apparently the correct blur length can not be computed with too may local minima

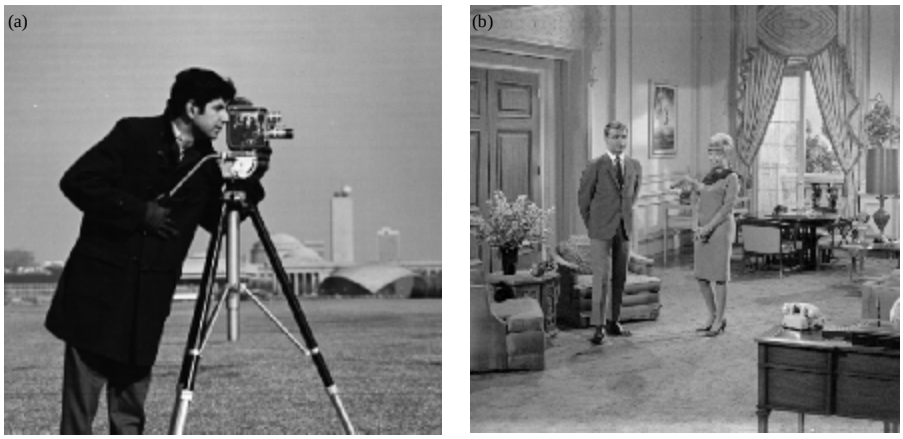

Fig. 5 (a-b): Additional two test images

Table 1: More experimental results with Lena. The blur lengths are randomly selected with blur directions equally separated by 5 degrees

True blur	Estimated blur	Error
(10, 60)	(10.0392, 59.7110)	(0.0392, 0.2890)
(11, 55)	(11.2527, 54.8327)	(0.2527, 0.1673)
(12, 50)	(12.3373, 50.5181)	(0.3373, 0.5181)
(17, 45)	(17.0667, 45.0000)	(0.0667, 0.0000)
(18, 40)	(17.9649, 40.5346)	(0.0351, 0.5346)
(20, 35)	(20.1173, 34.2304)	(0.1173, 0.7696)
(21, 30)	(20.7919, 30.3635)	(0.2081, 0.3635)
(25, 25)	(25.0980, 24.1392)	(0.0980, 0.8608)
(30, 20)	(29.8667, 19.3234)	(0.1333., 0.6766)
(35, 15)	(35.0316, 14.2295)	(0.0316, 0.7705)
(37, 10)	(37.0679, 9.7524)	(0.0679, 0.2476)

Table 2: Experimental results with the same blur kernels as Table 1 for Fig. 5a

True blur	Estimated blur	Error
(10, 60)	(10.2145, 60.1597)	(0.2145, 0.1597)
(11, 55)	(11.2527, 55.2379)	(0.2527, 0.2379)
(12, 50)	(12.3373, 50.4434)	(0.3373, 0.4434)
(17, 45)	(17.0667, 45.2938)	(0.0667, 0.2938)
(18, 40)	(17.9649, 39.7430)	(0.0351, 0.2570)
(20, 35)	(20.2772, 35.0012)	(0.2772, 0.0012)
(21, 30)	(20.8372, 30.0555)	(0.1628, 0.0555)
(25, 25)	(25.1288, 24.6411)	(0.1288, 0.3589)
(30, 20)	(29.9415, 19.9743)	(0.0585, 0.0257)
(35, 15)	(34.8299, 15.7316)	(0.1701, 0.7316)
(37, 10)	(36.7590, 10.1451)	(0.2410, 0.1451)

Table 3: Experimental results with the same blur kernels as Table 1 for Fig. 5b

True blur	Estimated blur	Error
(10, 60)	(9.8733, 60.1980)	(0.1267, 0.1980)
(11, 55)	(11.0703, 55.1721)	(0.0703, 0.1721)
(12, 50)	(11.7029, 49.9009)	(0.2971, 0.0991)
(17, 45)	(16.9256, 44.2658)	(0.0744, 0.7342)
(18, 40)	(17.8605, 39.8074)	(0.1395, 0.1926)
(20, 35)	(20.1348, 34.7447)	(0.1348, 0.2553)
(21, 30)	(21.1134, 29.8339)	(0.1134, 0.1661)
(25, 25)	(25.2217, 25.1698)	(0.2217, 0.1698)
(30, 20)	(29.7674, 19.6711)	(0.2326, 0.3289)
(35, 15)	(34.9814, 14.9557)	(0.0186, 0.0443)
(37, 10)	(36.9231, 10.2233)	(0.0769, 0.2233)

Figure 4 a-d shows the process of blur length computation for the image in Fig. 2a. In the collapsed 1D spectrum in Fig. 4c, averaging all minima together except the left-most and right-most ones, we can obtain the blur length 14.9851 which is very close the true value 15. We also try to collapse the binary image of the log spectrum in Fig. 4b but get many noisy local minima in Fig. 4d. It demonstrates that the blur length estimation using the log spectrum directly is better than using its binary image.

CONCLUSIONS

This study is on the linear motion blur estimation and presents an improvement to the frequency based method. The proposed method adopts a new preprocessing step where Hann windowing is used to remove boundary artifacts and histogram equalization is used to enhance contrast. The method also presents an improved Hough transform which adopts a least squares line fitting into the traditional Hough transform in the cepstrum domain to accurately estimate the motion direction. Experimental results show that this novel method is effective in the blur estimation.

For the future study, we will study more complex motion blur which is very difficult to estimate with existing reports (Whyte *et al*., 2010; Gupta *et al*., 2010). The patch-based method proposed by Schoueri *et al*. (2009) might be helpful for such a study. Deblurring such type of image to obtain a clear image is also very interesting and therefore, will also be researched in the future.

ACKNOWLEDGMENTS

The work is co-supported by National Natural Science Foundation of China (61003131, 61003038 and 61073116), Key Science Fund for Higher Education of Anhui Province (KJ2010A010), Key Science Fund for Young Researchers of Anhui University (2009QN009A) and Scientific Research Foundation for the Returned Overseas Chinese Scholars, State Education Ministry.

REFERENCES

Bai, L., F. Chen and X. Zeng, 2008. Application of markov random field in depth information estimation of microscope defocus image. Inform. Technol. J., 7: 808-813.

Boracchi, G., V. Caglioti and A. Giusti, 2008. Single-image 3d reconstruction of ball velocity and spin from motion blur-An experiment in motion-from-blur. Proceeding of the International Conference on Computer Vision Theory and Applications, Jan. 22-25, Funchal, Madeira, Portugal, pp: 22-29.

Cai, J.F., R.H. Chan and M. Nikolova, 2010. Fast two-phase image deblurring under impulse noise. J. Math. Imaging Vision, 36: 46-53.

Cannon, M., 1976. Blind deconvolution of spatially invariant image blurs with phase. IEEE Trans. Acoust. Speech Signal Process., 24: 58-63.

Dai, S. and Y. Wu, 2008. Motion from blur. Proceedings of the IEEE Conference on Computer Vision and Pattern Recognition, June 23-28, Anchorage, Alaska, USA., pp: 1-8.

Dobes, M., L. Machala and T. Furst, 2010. Blurred image restoration: A fast method of finding the motion length and angle. Digital Signal Process., 20: 1677-1686.

Gonzalez, R.C. and R.E. Woods, 2007. Digital Image Processing 3rd Edn., Prentice Hall, New York, ISBN-13: 9780131687288.

Gupta, A., N. Joshi, C.L. Zitnick, M. Cohen and B. Curless, 2010. Single image deblurring using motion density functions. Proceedings of the 11th European Conference on Computer Vision: Part I, Sept 5-11, Berlin, Heidelberg, pp: 171-184.

Iffa, E.D., A.R.A. Aziz and A.S. Malik, 2011. Gas flame temperature measurement using background oriented schlieren. J. Applied Sci., 11: 1658-1662.

Ji, H. and C. Liu, 2008. Motion blur identification from image gradients. Proceedings of the IEEE Conference on Computer Vision and Pattern Recognition, June 23-28, Anchorage, AK, pp: 1-8.

Lagendijk, R.L. and B. Jan, 2005. Basic Methods for Image Restoration and Identification. In: Handbook of Image and Video Processing, 2nd Edn., Elsevier Academic Press, Burlington, MA., ISBN-13: 9780121197926, pp: 167-181.

Lokhande, R., K.V. Arya and P. Gupta, 2006. Identification of parameters and restoration of motion blurred images. Proceedings of the ACM Symposium on Applied Computing, April 23-27, New York, USA., pp: 301-305.

Moghaddam, M.E. and M. Jamzad, 2007. Motion blur identification in noisy images using mathematical models and statistical measures. Pattern Recognit., 40: 1946-1957.

Qureshi, I.M., T.a. Cheema, A. Naveed and A. Jalil, 2003. Genetic algorithms based artificial neural networks for blur identification and restoration of degraded images. Inform. Technol. J., 2: 21-24.

Rav-Acha, A. and S. Peleg, 2005. Two motion-blurred images are better than one. Pattern Recognit. Lett., 26: 311-317.

Rekleitis, I.M., 1995. Visual motion estimation based on motion blur interpretation. Master's thesis, School of Computer Science, McGill University, Montreal, Quebec, Canada.

Richardson, W.H., 1972. Bayesian-based iterative method of image restoration. J. Opt. Soc. Am., 62: 55-59.

Schoueri, Y., M. Scaccia and I. Rekleitis, 2009. Optical flow from motion blurred color images. Proceedings of the Canadian Conference on Computer and Robot Vision, May 25-27 Kelowna, BC, Washington, DC, USA, pp: 1-7.

Whyte, O. J. Sivic, A. Zisserman and J. Ponce, 2010. Non-uniform deblurring for shaken images. IEEE Comput. Soc. Conf. Comput. Vision Pattern Recognit., 2010: 491-498.

Yitzhaky, Y. and N.S. Kopeika, 1997. Identification of blur parameters from motion blurred images. Graphical Models Image Process., 59: 310-320.

Yu, W.Z., H.X. Han, L.X. De, W. Min and Y.H. Cheng, 2008. A simultaneous localization and mapping method based on fast-hough transform. Inform. Technol. J., 7: 190-194.

Yu, X., Y. Gao, X. Yang, C. Shi and X. Yang, 2010. Image restoration method based on least-squares and regularization and fourth-order partial differential equations. Inform. Technol. J., 9: 962-967.